

# Energy absorption efficiency of carbon fiber reinforced polymer laminates under high velocity impact



Bing Wang<sup>a,b,\*</sup>, Jian Xiong<sup>a</sup>, Xiaojun Wang<sup>a</sup>, Li Ma<sup>a</sup>, Guo-Qi Zhang<sup>a</sup>, Lin-Zhi Wu<sup>a</sup>, Ji-Cai Feng<sup>b</sup>

<sup>a</sup> Center for Composite Materials, Harbin Institute of Technology, Harbin 150001, PR China

<sup>b</sup> School of Materials Science and Engineering, Harbin Institute of Technology, Harbin 150001, PR China

## ARTICLE INFO

### Article history:

Received 9 October 2012

Accepted 23 January 2013

Available online 14 March 2013

### Keywords:

Carbon fiber reinforced polymer

High velocity impact behavior

Energy absorption efficiency

Numerical model

## ABSTRACT

In this paper, response of carbon fiber reinforced polymer (CFRP) laminates subjected to high velocity impact has been investigated by experimental and numerical methods. Experiments using a two-stage light gas gun were conducted to investigate the impact process and to validate the finite element model. The energy absorption efficiency (EAE) of CFRP laminates with different thickness was investigated. According to the results of experiments and numerical calculations, thin CFRP laminates have a good EAE under relative higher velocity impact; by contraries, a superior EAE is displayed in thick laminates under relative lower velocity impact. Subsequently, EAE of CFRP laminates was compared with that of 304 stainless-steel plates. In a specific impact velocity range, EAE of CFRP laminates is higher than that of 304 stainless-steel. Thus, CFRP laminates have a potential advantage to substitute the metal plates to be used in high velocity impact resistance structures under a specific impact velocity range.

© 2013 Elsevier Ltd. All rights reserved.

## 1. Introduction

Carbon fiber reinforced polymer (CFRP) laminates are commonly used in lightweight constructions especially in aerospace industries due to the high specific strength and stiffness. As structural materials used in aerospace, it is important to evaluate their impact perforation behavior at the impact velocity of about 1000 m/s. Compared with damage in low velocity impact, the damage in the high velocity impact is more localized and does not depend on size of the target [1,2]. Tanabe et al. [3,4] have investigated the behavior of CFRP laminates damaged by the impact of a steel sphere. The stress and stress-time histories on the specimens were strongly affected by the type of carbon fiber and the interface strength of fiber/matrix. Interestingly, they have not observed obvious difference in the high velocity impact performance of cross-ply laminates and woven cloth. Hammond et al. [5–7] have investigated the impact deformation of CFRP laminates with different lay-ups. Unidirectional composites exhibited anisotropic behaviors and were significantly weaker than the other lay-ups. The crack can propagate across the samples with unidirectional lay-ups easily as expected.

In the research on perforation mechanisms, numerous ballistic tests were performed. Hazell et al. [8] has previously shown that below the impact energy of 500 J, the energy absorbed by 3 mm

and 6 mm woven CFRP plates dropped off and appeared to approach an asymptotic level. Subsequently, Hazell et al. [9] investigated the impact responses of 6-mm thickness woven CFRP plates subjected to impact by a steel sphere up to the velocity of 1875 m/s. It was observed that the above threshold impact energy, the percentage of kinetic energy dissipated by the laminate was constant. Further, the level of damage measured by C-Scan and through-thickness microscopy remained roughly constant as the impact energy increased. Fujii et al. [10] have investigated the impact property of several kinds of CFRP laminate specimens consisting of different carbon fibers, interlaminar sequences, configurations and thicknesses. They observed a ‘fluid-like’ failure of the laminate. They also demonstrated that the delamination width depended on impact energy. Hosur et al. [11] have carried out the high-velocity impact tests up to perforation on stitched and unstitched panels. The damage in the stitched samples was smaller than damage in the unstitched samples. However, the stitched plates displayed a lower ballistic resistance. Larsson [12] has also conducted ballistic tests on stitched and unstitched CFRP laminate. The results revealed the damage was reduced in the sewed panels. In order to determine the damage resistance of thin walled composite structures subjected to ice impact, Kim et al. [13] have performed high velocity impact experiments on woven carbon/epoxy panels. Moreover, the simulation was also conducted using spherical-shaped ice as hailstones. It can be obtained from experimental results that the kinetic energy initiating failure displays a linear relationship with the thickness of panel.

\* Corresponding author at: Center for Composite Materials, Harbin Institute of Technology, Harbin 150001, PR China. Tel.: +86 451 86402376.

E-mail address: [wangbing86@hit.edu.cn](mailto:wangbing86@hit.edu.cn) (B. Wang).

**Table 1**

Material property of T 700/epoxy laminate.

Property	Value
T700	
Longitudinal stiffness, $E_{11}$ (GPa)	132
Transverse stiffness, $E_{22}$ (GPa)	10.3
Out-of-plane stiffness, $E_{33}$ (GPa)	10.3
Poisson's ratio, $\nu_{12}$	0.25
Poisson's ratio, $\nu_{31}$	0.25
Poisson's ratio, $\nu_{23}$	0.38
Shear moduli, $G_{12}$ (GPa)	6.5
Shear moduli, $G_{13}$ (GPa)	6.5
Shear moduli, $G_{23}$ (GPa)	3.91
Longitudinal tensile strength, $X_t$ (MPa)	2100
Longitudinal compressive strength, $X_c$ (MPa)	1050
Transverse tensile strength, $Y_t$ (MPa)	24
Transverse compressive strength, $Y_c$ (MPa)	132
Interlaminar shear strength, $S$ (MPa)	75
Out-of-plane tensile strength, $Z_t$ (MPa)	65
Density, $\rho$ (kg/m <sup>3</sup> )	1570

A lot of analysis and numerical works were conducted in [14–21]. Lopez et al. [22] have developed an analytical model to predict the residual velocity of a steel projectile after penetrating through a woven carbon/epoxy laminate. The model considered three different energy absorption mechanisms for the laminate: linear momentum transfer, fiber failure and laminate crushing. Using ABAQUS, Lopez et al. [23] have presented a finite element model to predict the residual velocity and damaged area for woven carbon/epoxy laminates subjected to high impact velocities (velocity up to 550 m/s). Experiments using a gas gun were conducted to investigate the impact process and to validate the model. A morphology analysis was also made to investigate the different breakage mechanisms during the penetration process. In addition, the influence of the impact velocity/obliquity was studied using the numerical tool. A wide range of impact velocities and two impact angles, 0° and 45° were conducted in the calculations.

In this paper, the response of CFRP laminates impacted by a low mass steel sphere projectile with high velocity has been investigated by experiments and numerical calculations. Two different damage modes have been observed under different impact veloci-

ties. In order to explore the effect of thickness for the energy absorption efficiency (EAE), two CFRP laminates in different thickness have been investigated. EAE in 3 mm thick CFRP laminates is compared with that in 304 stainless steel plates with the same thickness. An optimized multilayer protection structure is designed, which is lighter compared with the traditional metal protection structure under the same protection effect.

## 2. Experimental investigation

### 2.1. Materials used

The materials used for investigation in this paper are carbon fiber reinforced polymer composites (T700/3234 Epoxy). All CFRP laminates are reinforced by means of T700 carbon fiber. The resin is 3234 epoxy system cured for 90 min at 130 °C and at a pressure of 0.5 Mpa. The mechanical properties of the unidirectional laminates are listed in Table 1. The volume fraction of carbon fiber is  $60.2 \pm 1.5\%$ . CFRP laminates with thickness of 3 mm and 1.5 mm are made from 36 plies and 18 plies, respectively. Only [0/90] symmetrical stacking sequence is selected in the study. The density of CFRP laminates is 1570 kg/m<sup>3</sup>, which is much smaller than that of 304 stainless steel (about 7800 kg/m<sup>3</sup>).

### 2.2. High velocity impact experiment

The ballistic performance of CFRP laminates is investigated by projectile impact velocities of 656, 757, 1137 and 1480 m/s according to the standard NATO STANAG-2920 [24]. Impact experiments were performed on 3 mm and 1.5 mm thick CFRP laminates, respectively. The size of impact samples was 100 mm × 100 mm. In all cases, CFRP laminates were impacted at mid-span by steel spherical, the projectile with a diameter of 6.0 mm and a weight of  $0.90 \pm 0.05$  g.

High velocity impact test was conducted by a two-stage light gas gun. The steel sphere was firstly accelerated from approximate 180 m/s to 2000 m/s by the gas gun. Then it was ejected from its launcher tube. Fig. 1 shows the photo and the schematic

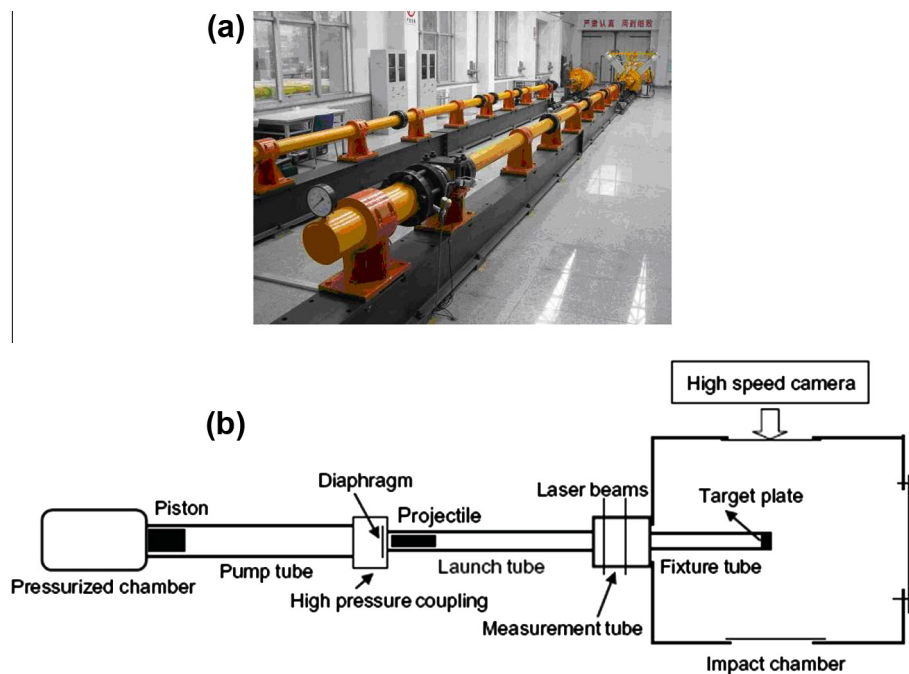


**Fig. 1.** The high velocity impact test device. (a) Photo of two-stage light-gas gun; (b) the sketch of the two-stage light-gas gun.

illustration of the test set-up used in this study. The gun mainly consisted of a pressurized chamber, a 57 mm caliber diameter nitrogen pump tube, a 12.7 mm caliber diameter with 3 m long launch tube, an impact chamber, and a measurement tube. The measurement tube had a 0.5 m free flight and the tube offered a space to have the initial velocity measure device installed. Beyond this, the tube connected the launch tube, the impact chamber and the fixture tube, which provided a support to the target plates. The striking velocity was controlled by the pressured gas (pressure and kinds of gas: hydrogen/nitrogen) and through the selection of the diaphragm material (steel or aluminum) as well as its thickness. One couple of lasers placed at the muzzle of the launch tube was used to trigger the timing device and to get the exit velocities. High-speed photography was used to observe the dynamic transverse deformation and failure of CFRP laminates. An Imacon 200 digital framing camera was used for this purpose; this camera was capable of capturing  $16 \times 10^6$  fps at a maximum rate of  $108 \times 10^6$  fps. In addition, the CFRP laminates were examined after each experiment to understand the failure mechanisms.

The sample test fixture was located within a blast chamber. A square, 40-cm-long, 2.86-cm-thick steel plate was located 1 m from the end of the launcher tube. It had a square hole with 70 mm long located in the center through which the projectile en-

tered the test area. A pair of brake screens was used to measure the projectile entry velocity with a precision of 2 m/s. Exit velocity was calculated by pictures which were recorded by high-speed photography. The test samples were clamped along all edges with the effective span of 70 mm  $\times$  70 mm.

### 3. Experimental results

#### 3.1. Perforation mechanisms

A sequence of high-speed photographs of the deformation and failure modes associated with the impact of the spherical projectile against the 1.5 mm thick CFRP laminates are included in Fig. 2 for projectile velocity of 1480 m/s. The photographs also confirm the impact position of the plates with the white circles. As the projectile velocity was high, a detached shock wave formed in front of the incoming projectile along with the bright patches associated with the ionization of air as the shock wave reflected off the plates.

There seem to be two distinct regimes in the reflected shock: (i) a dark cloud adjacent to the proximal face sheet immediately emerged; we believe that this cloud was caused by tiny fragments associated with the shear failure of the face sheet, and (ii) strong

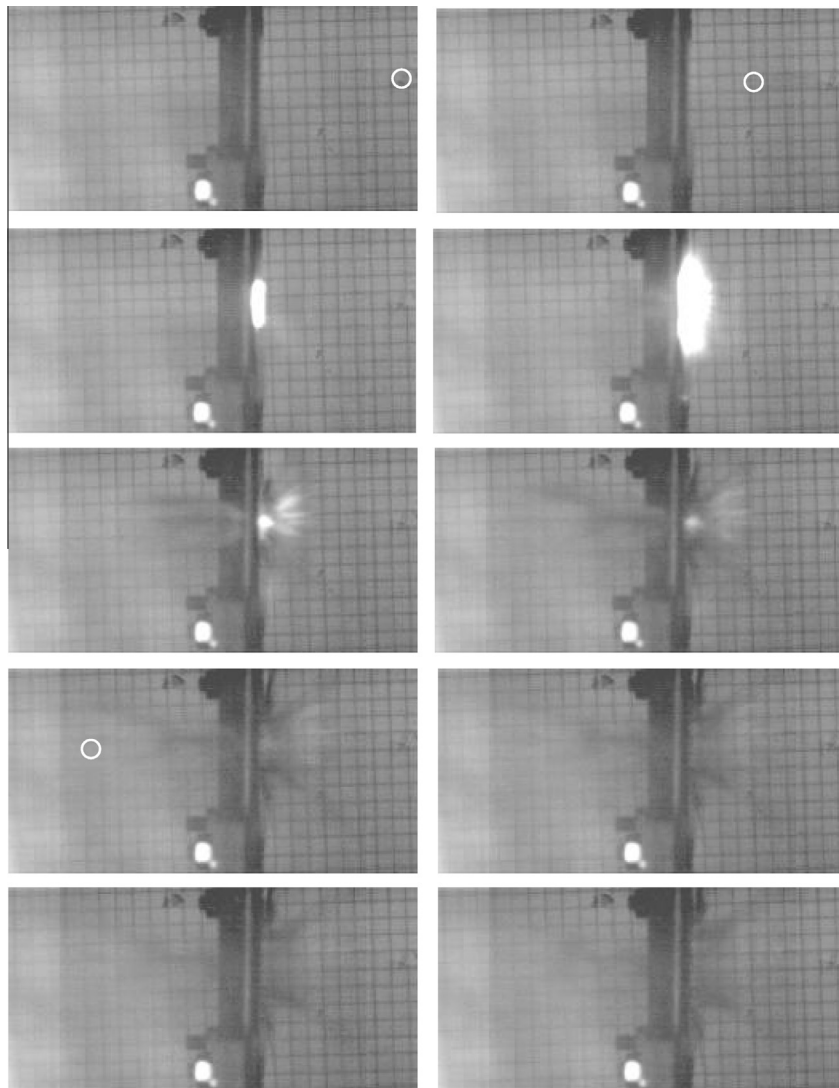


Fig. 2. High-speed photographs of carbon fiber laminate composites (1480 m/s).

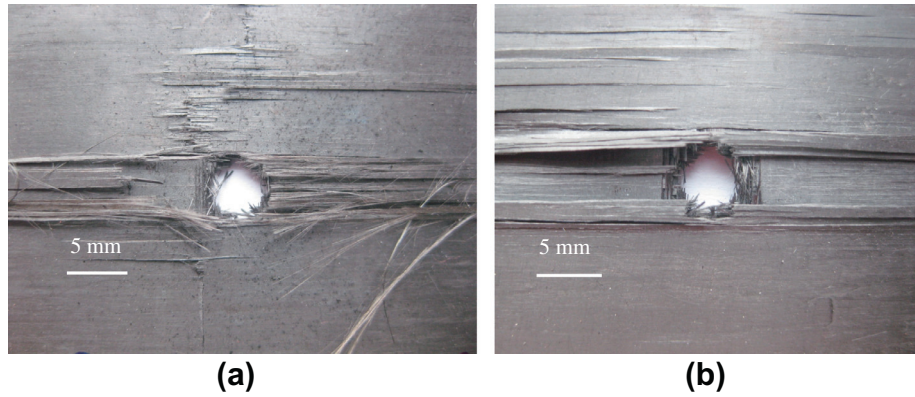


Fig. 3. Fracture carbon fiber laminates under high velocity impact (1480 m/s). (a) Front face; (b) back face.

reflected air shock where the density of the air rises sufficiently to cause a significant change in the refractive index of the air.

Photographs of the deformation and failure mechanisms of CFRP laminates are included in Figs. 3 and 4 for two selected projectile velocity. At  $V_p = 1480$  m/s, penetration of the laminate resulted in an entry hole approximately 6.48 mm in diameter, the plates failed in a shear-off mode. At  $V_p = 757$  m/s, the projectile penetrated the plates by shear-off and tensile tearing, and the failure in the back around the impact area were tensile fracture characteristics of fibers, as shown in Fig. 4b. However, in contrast with the impact velocity  $V_p = 1480$  m/s, the diameter of the hole in this case was greater than that of the projectile, with the diameter of the entry hole of 6.1 mm. This mode is known as ductile hole enlargement [13]: the observed thickening of the plate around the failure surface was associated with this hole enlargement process. The reduction in projectile velocity by this shear-off mechanism caused a sufficient reduction in the projectile velocity so that tensile tearing was again the operative failure mode for the distal face.

### 3.2. EAE in CFRP laminates

The measured projectile residual velocities  $V_r$  in two different thicknesses of CFRP laminates as a function of the initial impact velocity  $V_p$  are plotted in Fig. 5a. It can be seen from Fig. 5a that residual velocities in thick CFRP laminates are obviously smaller than that in thin CFRP laminates. Meanwhile, thick CFRP laminates can absorb more impact energy. However, high energy absorption in thick CFRP laminates is obtained at the cost of high mass (compared with thin CFRP laminates). It cannot be concluded that

energy absorption of thick CFRP laminates is better than that in thin CFRP laminates. So, EAE is defined as:

$$\eta = \frac{\frac{1}{2}M(V_p^2 - V_r^2)}{\frac{1}{2}MV_p^2 m} = \frac{(V_p^2 - V_r^2)}{mV_p^2} \quad (1)$$

Consequently, EAE is selected to evaluate the energy absorption in CFRP laminates. In Eq. (1),  $M$  is mass of the projectile;  $m$  is per unit area mass of CFRP laminates defined as:

$$m = \rho h \quad (2)$$

where  $\rho$  is density of CFRP laminates and  $h$  is thickness of CFRP laminates. Since high velocity impact behavior is highly localized and does not depend on the size of the target [1,2,25], per unit area mass of CFRP laminates  $m$  is selected to substitute the total mass of CFRP laminates. Substituting Eq. (2) into Eq. (1) gives:

$$\eta = \frac{(V_p^2 - V_r^2)}{\rho h V_p^2} \quad (3)$$

Substituting experimental results into Eq. (3), EAE in CFRP laminates with different thickness are plotted in Fig. 5b. In lower velocity (energy) impact, higher EAE are observed in both CFRP laminates, since failure mode is dominated by tension fracture. Under this tensile failure mode, thick CFRP laminates exhibit higher EAE in spite of their bigger mass. The reason of this result is that more fibers take the tensile resistance in thickness direction [1,9], which can compensate the negative effect by bigger mass. With the impact velocity (energy) increasing, damage mode in CFRP laminates gradually turned to shearing domination. Velocity of projectile cannot be reduced by fiber tensile resistance in CFRP laminates, so EAE in both CFRP laminates rapidly decreased.

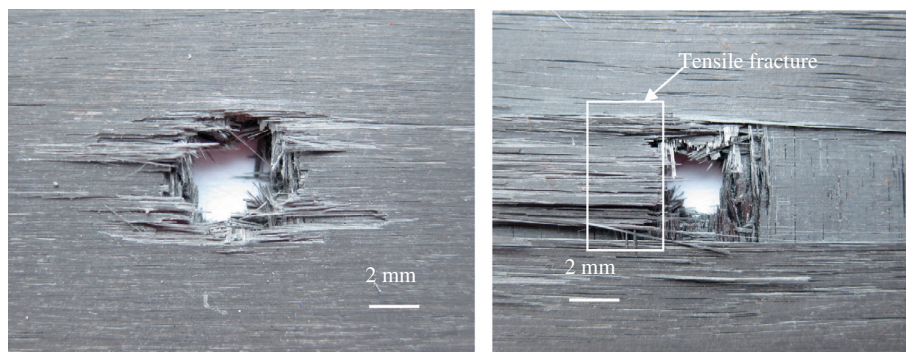


Fig. 4. Fracture of carbon fiber laminates under high velocity impact (757 m/s). (a) Front face; (b) back face.

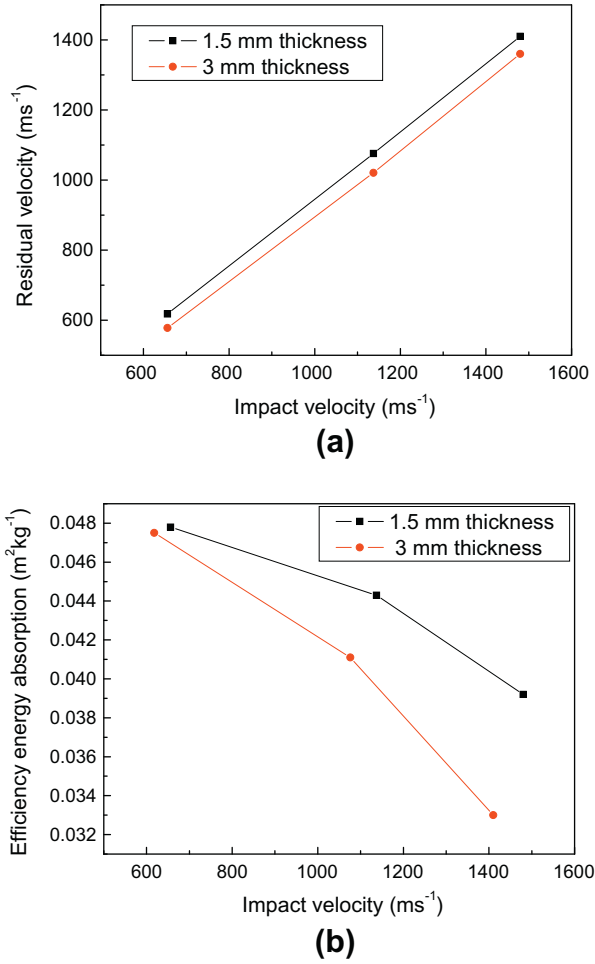


Fig. 5. Impact test results of carbon fiber composite laminates with different thickness: (a) relationship of residual velocity and impact velocity and (b) relationship of efficiency energy absorption and impact velocity.

#### 4. Numerical model

The explicit finite element software, ABAQUS/Explicit, was employed for impact simulation. The CFRP laminates are modeled as square plates, and clamped at all edges to simulate the clamped condition in test, as shown in Fig. 6. The CFRP laminates were meshed with 8-node linear reduced integration solid elements (C3D8R). Due to the poor aspect ratio of these elements, a reasonably fine mesh is required to ensure convergence. A graded mesh was thus created, where the region in the vicinity of the projectile was more finely meshed. Convergence calculation was conducted to ensure that the mesh refinement in CFRP laminates was sufficiently fine enough to capture the stresses and deformations with a reasonable accuracy. The calculation demonstrated that reasonable number in the contact area of each ply was  $40 \times 40$ , with one element per ply. Finally, the spherical steel projectile with diameter of 6 mm was also modeled using 8-node linear reduced integration solid elements (C3D8R). Ideally elastic–plastic constitutive relationship was employed for the property of steel projectile [26].

In order to simulate the damage of CFRP laminates under high velocity impact, a progressive damage model, which integrated stress analysis, failure analysis and material property degradation, was implemented in ABAQUS/Explicit using a user subroutine (VUMAT). The stress-based Hashin [27] and Chang–Chang [28,29]

criteria were used to detect four failure modes in the matrix and fiber: for matrix tensile or shear crack:

$$\frac{(\sigma_{yy} + \sigma_{zz})^2}{Y_t^2} + \frac{\sigma_{yz}^2 - \sigma_{yy}\sigma_{zz}}{S^2} + \frac{\sigma_{xy}^2 + \sigma_{xz}^2}{S^2} = 1, \quad (\sigma_{yy} + \sigma_{zz}) \geq 0 \quad (4)$$

$$\begin{aligned} & \frac{1}{Y_c} \left[ \left( \frac{Y_c}{2S} \right)^2 - 1 \right] (\sigma_{yy} + \sigma_{zz}) + \frac{(\sigma_{yy} + \sigma_{zz})^2}{4S^2} \\ & + \frac{\sigma_{xy}^2 + \sigma_{xz}^2 + \sigma_{yz}^2 - \sigma_{yy}\sigma_{zz}}{S^2} \\ & = 1, \quad (\sigma_{yy} + \sigma_{zz}) < 0 \end{aligned} \quad (5)$$

for fiber tensile failure:

$$\frac{\sigma_{xx}}{X_t} + \left( \frac{\sigma_{xy}^2 + \sigma_{xz}^2}{S^2} \right) = 1 \quad (6)$$

for fiber compressive failure:

$$\frac{\sigma_{xx}}{X_c} = 1 \quad (7)$$

for delamination:

$$\left( \frac{\sigma_{zz}}{Z_t} \right)^2 + \frac{\sigma_{xz}^2 + \sigma_{yz}^2}{S^2} = 1 \quad (8)$$

where the  $\sigma_{xy}$  terms are components of the stress tensor.  $x$  and  $y$  are local coordinate axes parallel and transverse to the fibers in each ply, respectively. The  $z$ -axis coincides with the through-thickness direction. In the present paper, failure criteria damage rules (Eqs. (4)–(8)) were employed to detect the damage in elements. Under a given load, the stresses at each integration point in the CFRP laminates were computed in the user subroutine. Then, the stresses were substituted into the failure criteria to evaluate the failure initiation. When the failure criterion was verified, the stresses in the damaged area were reduced close to zero. The material property degradation and stress update depended on the failure mode:

Matrix tensile cracking :  $E_{22} = \nu_{12} = 0$ ;

Matrix compressive failure :  $E_{22} = \nu_{12} = 0$ ;

Fiber tensile failure : Element delete;

Fiber compressive failure : Element delete;

Delamination :  $E_{33} = G_{13} = G_{23} = \nu_{23} = \nu_{13} = 0$ .

#### 5. Results and discussion

##### 5.1. Comparison between numerical results and experimental data

The impact responses of the CFRP laminates with different thickness were investigated by numerical method and the results are compared with experimental measurement, as shown in Fig. 7. It can be seen that the numerical methods can predict the high velocity impact response of CFRP laminates with different thickness. Different from low-velocity damage, the damage in CFRP laminates is localized under the high velocity impact, as shown in Fig. 8.

##### 5.2. Comparison of EAE between CFRP laminates and metal plates

Because of the excellent ductility, metal plates have been widely used for energy absorber. By contraries, CFRP laminates are not suitable as energy absorption materials due to their bad

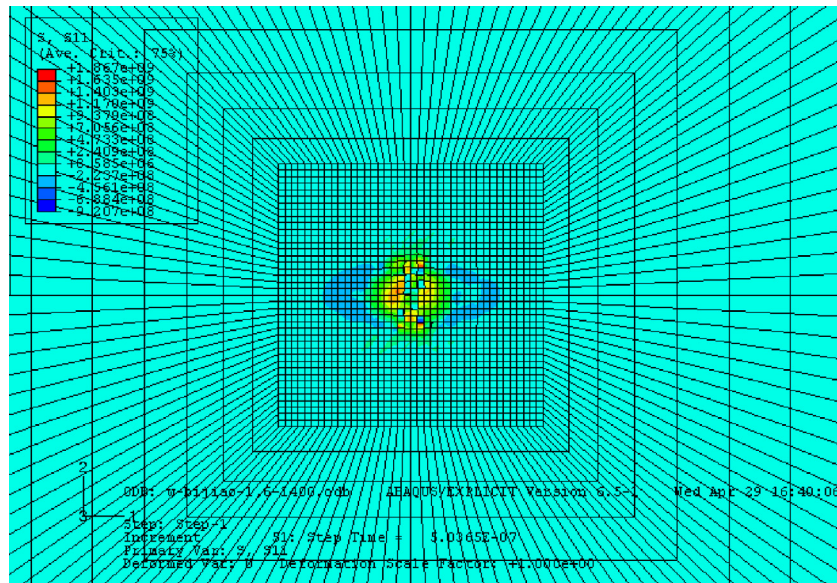


Fig. 6. FE model of carbon fiber composite laminates.

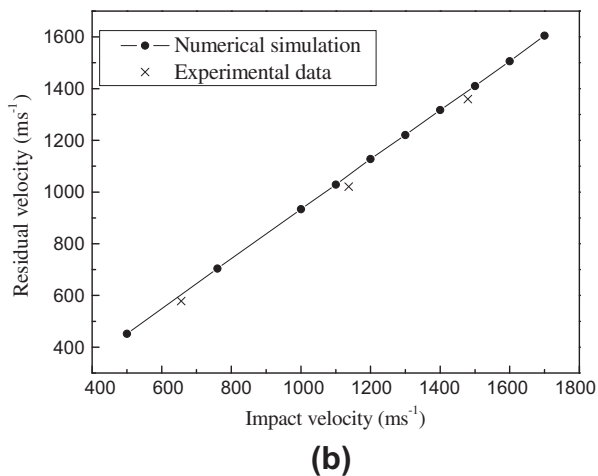
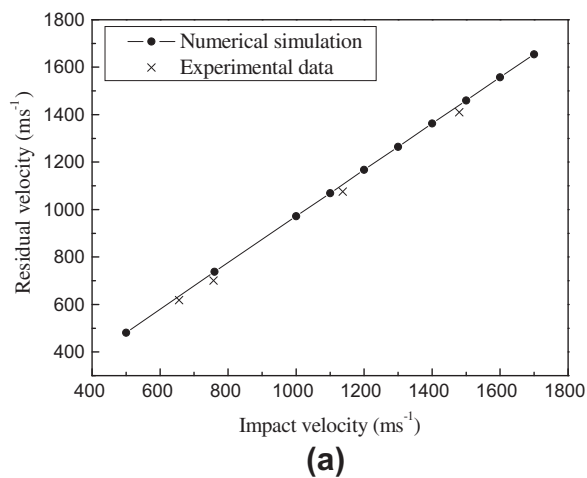


Fig. 7. Comparison between experimental results and numerical data of carbon fiber laminates under high velocity impact: (a) 1.5 mm thickness; (b) 3 mm thick.

ductility compared with metal plates in the traditional concept. The purpose of this section is to compare the EAE of CFRP laminates and metal plates, and show CFRP laminates can be used

as energy absorption structures under specific impact velocity (energy) range. It can be seen from Section 3.2 that EAE depends on the thickness of plates. Therefore, the comparison of EAE between CFRP laminates and metal plates must be conducted in same thickness. Compared with metal materials, EAE of CFRP laminates (calculated from FEM, the property of projectile is same with that used in [30]) under high velocity impact is higher than that in 304 stainless steel plates (result from [30]) under specific impact energy range, as shown in Fig. 9. There are two reasons for this result. First, the main damage mode in 304 stainless steel plates is shear failure under higher velocity (energy) impact, which induces a highly localized response in the target [30]. Due to the rapid penetration of the projectile through the steel plates in this shear-off failure mechanism, there is negligible associated plastic bending or stretching of the plates. Thus, under shear failure damage mode, 304 stainless steel plates cannot absorb more impact energy. The second reason is high density of 304 stainless steel (CFRP laminates have a density approximately one-fifth of steel) giving a negative effect on EAE. Although the failure mode is also shear-off for CFRP laminate under the high velocity impact and the absorbed energy of CFRP laminates decreases with the impact velocity increasing, considering the low density of CFRP material, the reduction of EAE for CFRP laminate is still smaller than that of metal plates. In view of these, EAE in CFRP laminates will be higher than that in 304 stainless steel plates under higher velocity (energy) impact, especially when the impact velocity is higher than 950 m/s. Although shear-off and tensile tearing were the failure mode of CFRP under low velocity (energy) impact, the absorbed energy was also added. With the impact velocity (energy) decreasing, the damage mode in 304 stainless steel plates is turning to plastic bending and stretching [30]. This leads to the plates can absorb much more energy than CFRP plates, which can compensate for the higher density of metal. Thus, in spite of relative high density, the EAE in 304 stainless steel plates exceeds the CFRP laminates under lower velocity (energy) impact, as shown in Fig. 8. In conclusion, 304 stainless steel plates are excellent energy absorber under lower velocity (energy) impact and CFRP laminates can replace 304 stainless steel plates as energy absorption structures under higher velocity (energy) impact, especially when the impact velocity is higher than 950 m/s.

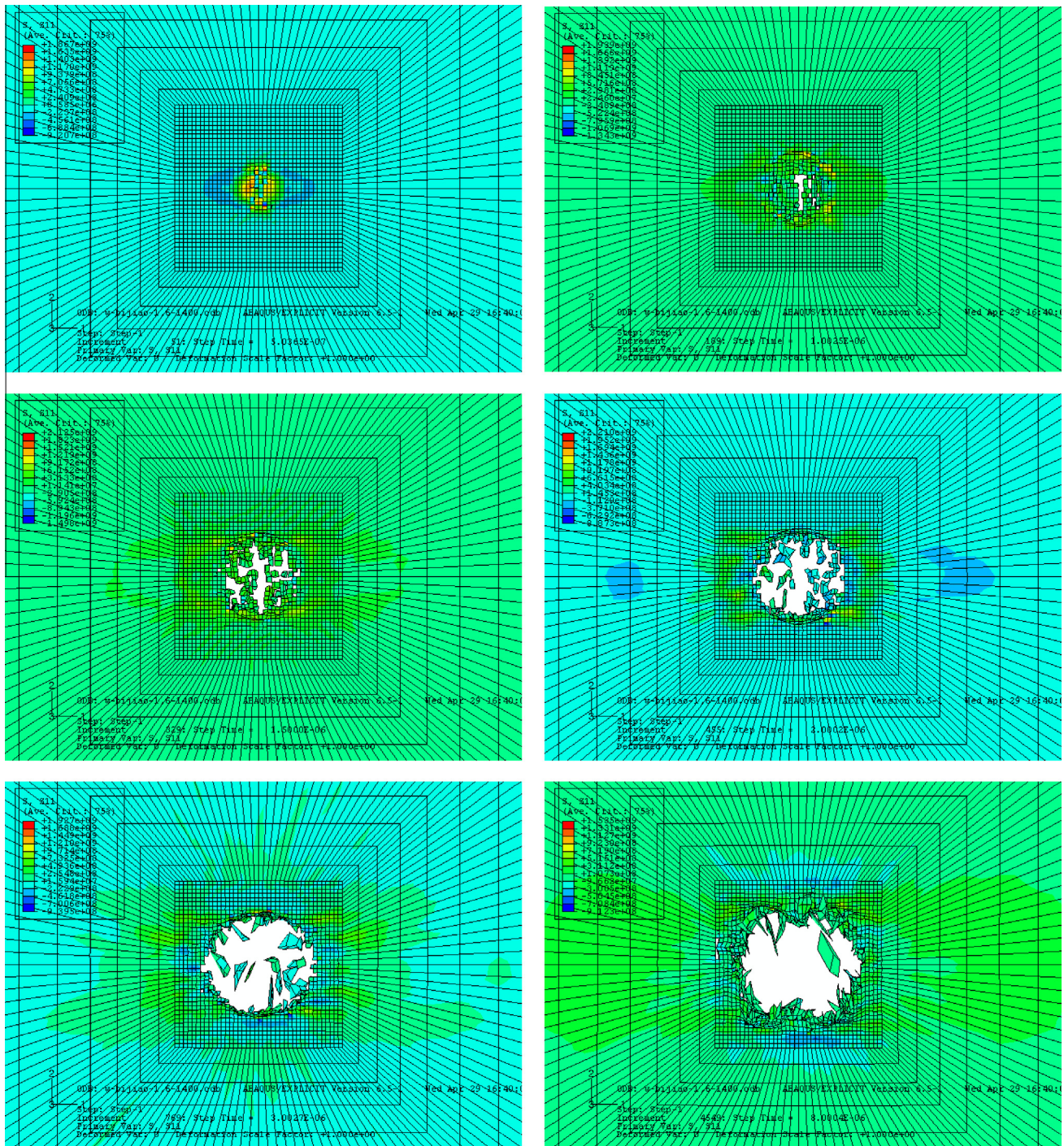


Fig. 8. FE results of carbon fiber composite laminates under high velocity impact with 1000 m/s.

### 5.3. Enhancement of EAE in CFRP laminates

EAE of CFRP laminates has been discussed in Section 3.2 by experimental method. In order to compare the EAE of CFRP laminates with different thickness, CFRP laminates with three different thicknesses (2, 2.4 and 2.8 mm) subjected to high velocity impact are calculated by numerical model, and the result is shown in Fig. 10. From Fig. 10 we can observe that the CFRP laminates of bigger thickness have the highest EAE when the impact velocity is lower than 650 m/s, and have the lowest EAE when the impact velocity is higher than 1188 m/s. In contrast, the CFRP laminates

of lower thickness have the lowest EAE when the impact velocity is lower than 650 m/s, and have the highest EAE when the impact velocity is higher than 1188 m/s.

When the impact velocity varies between 650 m/s and 950 m/s, the maximal EAE is obtained by 2.4 mm CFRP laminates and minimal EAE is obtained by 2 mm CFRP laminates. When the impact velocity varies between 950 m/s and 1188 m/s, the maximal EAE is obtained by 2.4 mm CFRP laminates and minimal EAE is obtained by 2.8 mm CFRP laminates.

In a word, thick CFRP laminates are appropriately used in lower velocity impact (energy), thin CFRP laminates are appropriately

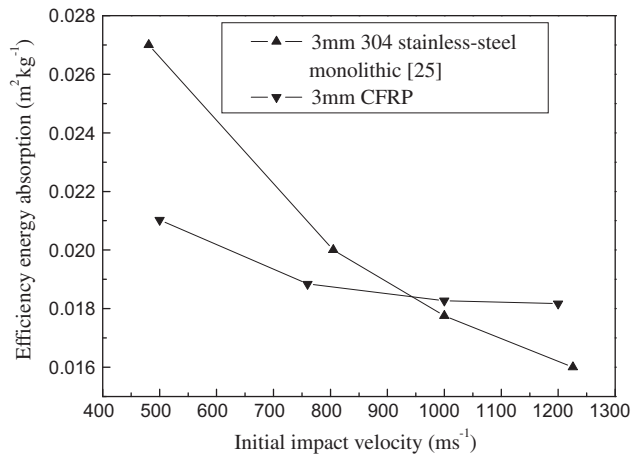


Fig. 9. Comparisons of energy absorption efficiency between CFRP laminate and stainless-steel monolithic plates.

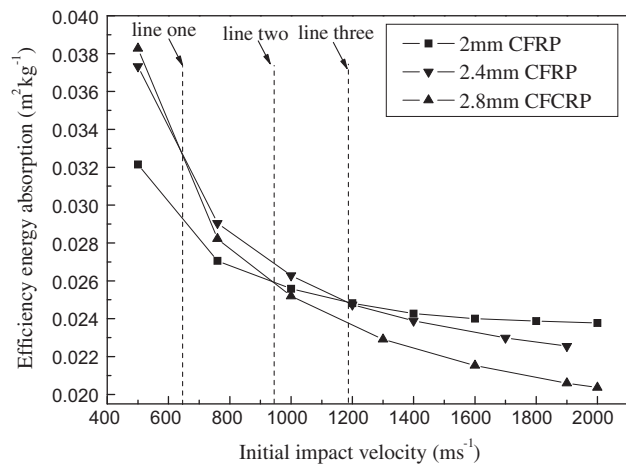


Fig. 10. Efficiency of energy absorption with different thicknesses.

used in higher velocity impact (energy), and CFRP laminates with moderate thickness are appropriately used when impact velocity (energy) is also moderate. Therefore, much better energy absorption can be obtained under the same total thickness of CFRP laminates by arranging different thinner CFRP laminates reasonably. One 4 mm thick CFRP laminates and two 2 mm CFRP laminates impacted with initial velocity of 3000 m/s are calculated by numerical model. The residual velocity is 2784.6 m/s for the 4 mm CFRP laminates with initial impact velocity of 3000 m/s. While the residual velocity is 2777 m/s for the two 2 mm CFRP laminates (the total mass is equal). The reason of this result is that the thin CFRP laminates have bigger EAE under higher velocity (energy) impact. So, the absorbed energy in 4 mm CFRP laminates is less than that in two 2 mm CFRP laminates. It can be concluded that choosing CFRP laminates with different thickness reasonably according to impact velocity (energy) can improve energy absorption under the same mass.

#### 5.4. Optimized protection structure

Based on the previous discussion, it is clear that the metal plates have higher EAE when the impact velocity is lower, but vice versa for the CFRP laminates. Moreover, when the total mass is equal, many thin CFRP laminates have higher EAE than a thick CFRP laminate under the high velocity impact. Thus, an optimized protec-

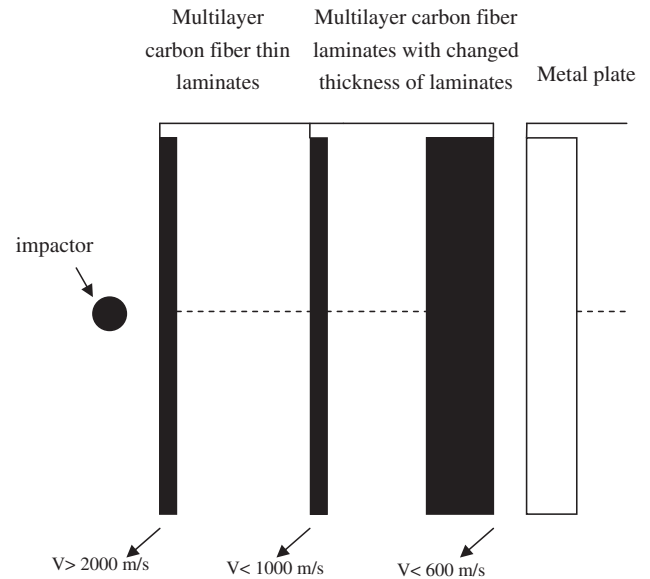


Fig. 11. Sketch map of optimized protection structure.

tion structure is designed as shown in Fig. 11. Multilayer thin CFRP laminates are placed outside, the thicker CFRP laminates are placed in the middle, and metal plates are placed inside.

As shown in Fig. 11, the bullet firstly impacts (impact velocity is higher than 2000 m/s) the peripheral protection structure (multilayer thin CFRP laminates), with the result of the impact velocity will be reduced to less than 1000 m/s after perforation. Then the impact velocity will be reduced to less than 600 m/s after perforation multilayer CFRP laminate with changed thickness. Following that, metal plates may be used to absorb the final energy. The optimized protection structure is lighter compared with the traditional metal protection structure when the protection effect is same.

## 6. Conclusion

In this paper, CFRP laminates subjected to high velocity impact with the velocity ranging from 180 to 2000 m/s have been investigated by experimental and numerical methods. Tensile failure mode and shearing failure mode are dominant in lower and higher velocity (energy) impact tests, respectively. According to experimental and numerical results, thin CFRP laminates have higher EAE under higher velocity (energy) impact; meanwhile, thick CFRP laminates have higher EAE under lower velocity (energy) impact. Based on numerical calculation and comparison, ballistic performance of 304 stainless steel plates is superior to CFRP laminates under the lower velocity impact. However, EAE in 304 stainless steel plates is exceeded by CFRP laminates under higher impact velocity (energy) because of the much higher density of metal. Therefore, CFRP laminates have a potential ability to replace the metal plates to act as energy absorption structures under higher velocity (energy) impact. Since EAE is different with the variation of CFRP laminates thickness, better energy absorption will be obtained under same mass by arranging CFRP laminates with the different thickness reasonably according to impact velocity (energy). Finally, an optimized protection structure, which contains multilayer thin CFRP laminates outside, multilayer CFRP laminates with changed thickness in the middle and the metal plate inside, is proposed. The optimized protection structure is lighter compared with the traditional metal protection structure when the protection effect is the same.

## Acknowledgements

The present work is supported by National Science Foundation of China under Grant No. 11202059, the Major State Basic Research Development Program of China (973 Program) under Grant No. 2011CB610303, the Fundamental Research Funds for the Central Universities Grant No. HIT. NSRIF. 2010069, the Natural Science Foundation of Heilongjiang Province, China (No. A201204), and Supported by Specialized Research Fund for the Doctoral Program of Higher Education of China (No. 2011230211006).

## References

- [1] Hazell PJ, Kister G, Stennett C, Bourque P, Cooper G. Normal and oblique penetration of woven CFRP laminates by a high velocity steel sphere. *Composites: Part A* 2008;39(5):866–74.
- [2] Cantwell WJ, Morton J. Impact perforation of carbon fiber reinforced plastic. *Compos Sci Technol* 1990;38(2):119–41.
- [3] Tanabe Y, Aoki M, Fujii K, Kasano H, Yasuda E. Fracture behavior of CFRPs impacted by relatively high-velocity steel sphere. *Int J Impact Eng* 2003;28(6):627–42.
- [4] Tanabe Y, Aoki M. Stress and strain measurements in carbon-related materials impacted by a high-velocity steel sphere. *Int J Impact Eng* 2003;28(10):1045–59.
- [5] Hammond RI, Proud WG, Goldrein HT, Field JE. High-resolution optical study of the impact of carbon-fibre reinforced polymers with different lay-ups. *Int J Impact Eng* 2004;30(1):69–86.
- [6] Will MA, Franz T, Nurick GN. The effect of laminate stacking sequence of CFRP filament wound tubes subjected to projectile impact. *Compos Struct* 2002;58(2):259–70.
- [7] Lopez-Puente J, Zaera R, Navarro C. The effect of low temperatures on the intermediate and high velocity impact response of CFRP. *Composites Part B* 2002;33(8):559–66.
- [8] Hazell PJ, Kister G, Bourque P, Cooper G. Normal and oblique penetration of woven CFRP laminates by a high velocity steel sphere. *Composites Part A* 2008;39(5):866–74.
- [9] Hazell PJ, Cowie A, Kister G, Stennett C, Cooper GA. Penetration of a woven CFRP laminate by a high velocity steel sphere impacting at velocities of up to 1875 m/s. *Int J Impact Eng* 2009;36(9):1136–42.
- [10] Fujii K, Aoki M, Kiuchi N, Yasuda E, Tanabe Y. Impact perforation of CFRPs using high-velocity steel sphere. *Int J Impact Eng* 2002;27(5):497–508.
- [11] Hosur MV, Vaidya UK, Ulven C, Jeelani S. Performance of stitched/unstitched woven carbon/epoxy composites under high velocity impact loading. *Compos Struct* 2004;64(3–4):455–66.
- [12] Larsson F. Damage tolerance of a stitched carbon/epoxy laminate. *Composites Part A* 1997;28(1):923–34.
- [13] Kim H, Welch DA, Kedward KT. Experimental investigation of high velocity ice impacts on woven carbon/epoxy composite panels. *Composites Part A* 2003;34(1):25–41.
- [14] Cantwell WJ, Morton J. Comparison of low and high velocity impact response of CFRP. *Composites* 1989;20(6):545–51.
- [15] Keisuke F, Motokazu A, Noriyuki K, Eiichi Y, Yasuhiro T. Impact perforation behavior of CFRPs using high-velocity steel sphere. *Int J Impact Eng* 2002;27(5):497–508.
- [16] Lopez-Puente J, Zaera R, Navarro C. An analytical model for high velocity impacts on thin CFRP woven laminates. *Int J Solids Struct* 2007;44(9):2837–51.
- [17] Lopez-Puente J, Zaera R, Navarro C. Numerical modelling of high velocity impact on CFRPs at low temperature. In: Fourteenth Dymat Technical Meeting. Sevilla, Spain; 2002. p. 121–9.
- [18] Reid SR, Wen HM. Impact behavior of fibre-reinforced composite materials and structures. Cambridge: Woodhead Publication; 2000. [Ch Perforation of FRP laminates and sandwich panels subjected to missile impact]
- [19] Chen JK, Allahdadi FA, Carney TC. High-velocity impact of graphite/epoxy composite laminates. *Compos Sci Technol* 1997;57(9–10):1369–79.
- [20] Ramadhan AA, Abu Talib AR, Mohd Rafie AS, Zahari R. High velocity impact response of Kevlar-29/epoxy and 6061-T6 aluminum laminated panels. *Mater Des* 2013;4:307–21.
- [21] Pandya Kedar S, Pothnis Jayaram R, Ravikumar G, Naik NK. Ballistic impact behavior of hybrid composites. *Mater Des* 2013;44:128–35.
- [22] Lopez-Puente J, Varas D, Loya JA, Zaera R. Analytical modelling of high velocity impacts of cylindrical projectiles on carbon/epoxy laminates. *Compos Part A* 2009;40(8):1223–30.
- [23] Lopez-Puente J, Zaera R, Navarro C. Normal and oblique penetration of woven CFRP laminates by a high velocity steel sphere. *Compos Part A* 2008;39(5):866–74.
- [24] NATO STAN AG-2920. Ballistic test method for personal armour materials and combat clothing. 2nd edition. NATO Standardization Agency; July 2003.
- [25] Lopez-Puente J, Zaera R, Navarro C. Experimental and numerical analysis of normal and oblique ballistic impacts on thin carbon/epoxy woven laminates. *Compos Part A* 2008;39(2):374–87.
- [26] Abaqus Explicit User's Manual. Version 6.5 Edition. HKS; 2005.
- [27] Hahin Z. Failure criteria for unidirectional fiber composites. *J Appl Mech* 1980;47:329–34.
- [28] Chang FK, Chang KY. Post-failure analysis of bolted composite joints in tension or shear-out mode failure. *J Compos Mater* 1987;21(9):809–33.
- [29] Chang FK, Chang KY. A progressive damage model for laminated composites containing stress concentrations. *J Compos Mater* 1987;21(9):834–55.
- [30] Christian J, Yungwirth, Wadley HNG, O'Connor JH, Zakraysek AJ, Deshpande VS. Impact response of sandwich plates with a pyramidal lattice core. *Int J Impact Eng* 2008;35(8):920–36.